# Event Driven Control of Voltage and Current Gradients of Medium Voltage IGBTs

***Abstract* – Medium voltage IGBTs are fast switching devices that require low gate drive power. They inherently generate high voltage and current gradients during switching transitions. These are generally limited by retarding the changes of the gate charge. Additional gate resistors are usually installed for this purpose. The drawback is high switching losses.**

**A novel method is described in this paper that aims at controlling the voltage and current gradients during switching transitions. The gate charge of the input MOS device is controlled by injected gate currents. These follow particular command functions that are predefined and stored in a memory. The method requires reacting within microseconds which traditional closed loop control cannot do. Specific time events are therefore defined to trigger the respective command function. These functions depend on the instantaneous values of the collector current or the collector-emitter voltage, variables that are identified without delay, knowing their predefined gradients and counting the time from the respective event to reach their final values.**

**Experimental results show the performance of event driven control. Low current and voltage gradients are enforced while the switching losses are reduced.**

## I. Introduction

Integrated gate bipolar transistors (IGBTs) are the preferred power semiconductor devices used for medium voltage inverters. Their fast switching transients are controlled through a MOS gate which requires only low control power. Typical applications are speed variable ac machine drives in the upper megawatt range.

The maximum ratings of presently available medium voltage IGBTs are $U_{CE\,max}$ = 6.5 kV and $I_{C\,max}$ = 750 A. These high values cause considerable device losses during switching transitions. Medium voltage inverters must be therefore operated at low switching frequencies of only few hundred Hertz in order to restrain the switching losses to tolerable levels [1]. Optimal pulsewidth modulation technics are then applied to keep the harmonic current distortion low. This can be achieved by synchronous optimal pulsewidth modulation [2], or alternatively by predictive current control [3]. An additional option is using multilevel inverter topologies that inherently produce lower current distortion [4].

While these methods provide low harmonic distortion at low switching frequency, two major problems that relate to the switching transitions remain unsolved:

• High *voltage gradient*s entail
  - insulation stress on the stator windings,
  - overvoltages due to travelling waves in the motor cable,
  - generation of bearing currents,
  - poor EMC compatibility.

• High *current gradient*s entail
  - high IGBT losses at turn on,
  - high diode losses at turn off.

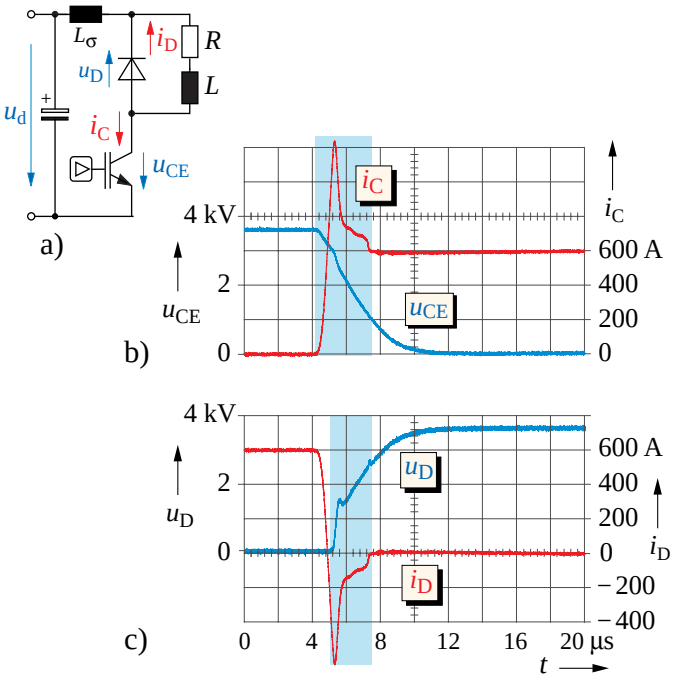


Fig. 1 Commutation waveforms: a) equivalent circuit, b) IBGT waveforms, c) diode waveforms. Device losses occur in the blue regions.

The effect of high current gradients is visualized in the commutation waveforms **Fig. 1**. Blue areas mark the regions where losses of IGBT and diode occur. The diode reverse recovery current of high amplitude reflects also on the IBGT.

Voltage and current gradients are conventionally limited by inserting an additional resistor at the gate terminal [5], [6]. The resistor delays the gradient of the gate voltage, and consequently the respective gradients of the collector emitter voltage and the collector current. Values of about 1 kV/$\mu$s and 2 kA/$\mu$s are a common target. The trade-off is higher commutation losses.

**Fig. 2** shows that a current gradient of 2.7 kA/$\mu$s at turn on leads to device losses of 3.2 Ws per commutation. A voltage gradient of 1 kV/$\mu$s at turn off produces 4.8 Ws per commutation, **Fig. 3**. An inverter operating at $f_S$ = 200 Hz switching frequency then generates losses of 15 kW per device. Heat

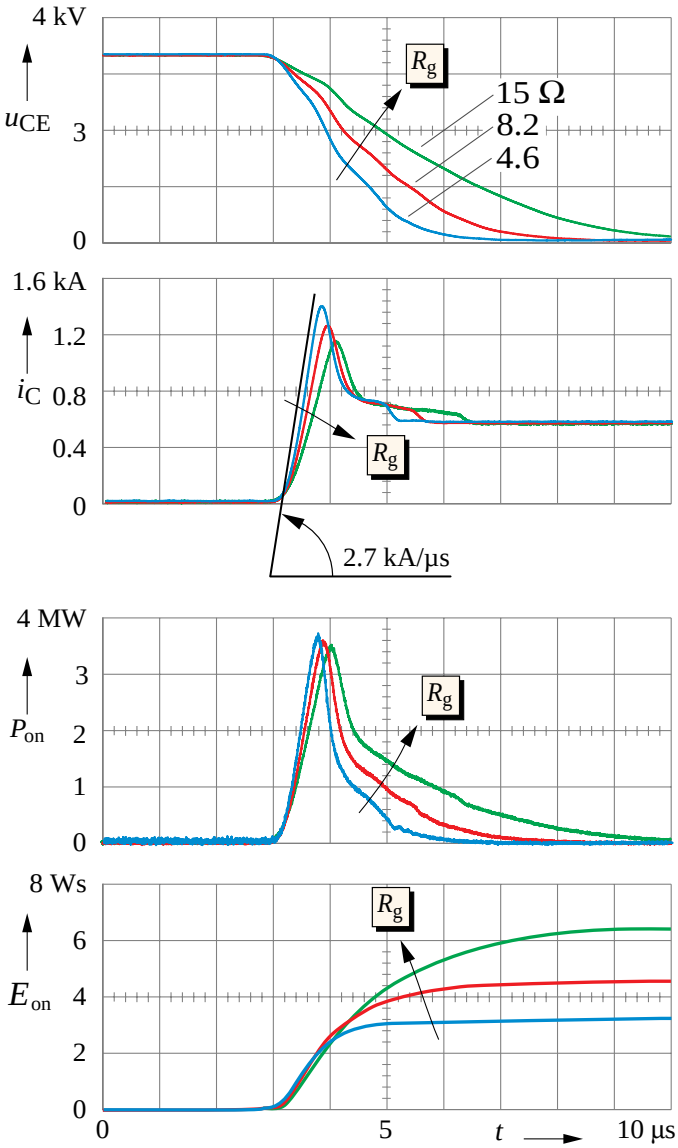


Fig. 2 Turn-on performance with different gate resitors $R_g$

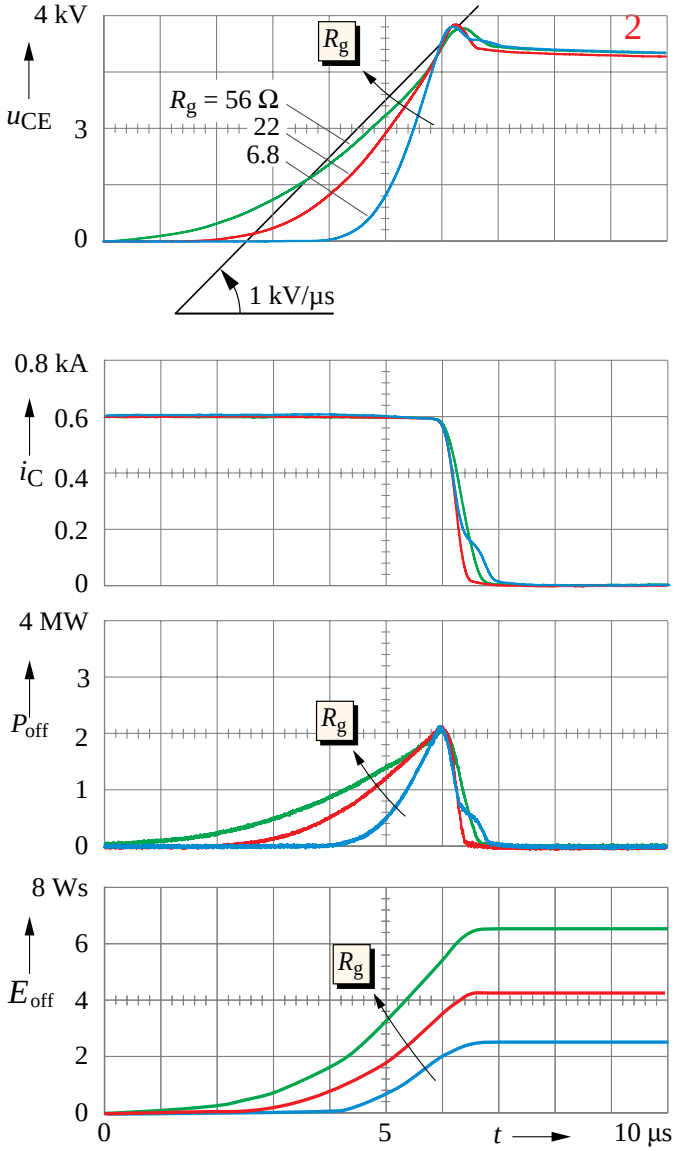


Fig. 3 Turn-off performance with different gate resitors $R_g$

dissipation becomes a problem such that the capability of the devices cannot be fully utilized. Operating at high gradients requiers installing expensive output filters to protect the motor against switching overvoltages and bearing currents [7].

Analytical models have been used to investigate the switching properties of IGBTs and to control the voltage gradient [6]. The interactions between the gate drive and the device are described in [8]. The results in [5, 6, 8] refer to low voltage IGBTs that operate at high switching frequencies. They are not applicable to medium voltage devices.

The method described in this paper aims at controlling the voltage and current gradients during switching transitions and make them to follow predefined reference values while simultaneously reducing the switching losses.

## II. IGBT Dynamics

IGBTs are conventionally described by a static model as shown in **Fig. 4(a)**. The signal flow graph Fig. 3(b) represents its dynamic behavior. Symbols displaying the step response are used here for characterization.

The input variable in Fig. 4(b) is the gate-emitter voltage $u_{GE}$ and the output variable is the collector current $i_C$. When a positive step of $u_{CE}$ is applied, the gate-emitter-capacitance $C_{GE}$ gets charged and the gate-emitter voltage $u_{GE}$ starts increasing. Eventually will this voltage reach the threshold voltage $u_{th}$ shown in Fig. 4(a). The collector current $i_C$ then begins to rise. The IGBT acts as a voltage controlled device in this mode.

The dynamic properties of the IGBT are derived from the equivalent circuit **Fig. 5**. The gate control signal acts upon a MOSFET structure which is the input device. The MOSFET generates the base current of a bipolar transistor which is the output device. A delay occurs during this process while the gate-emitter capacitance $C_{GE}$ gets charged through the internal gate resistor $R_{G\ int}$. Further delay occurs until the base-emitter voltage $u_{BE}$ has reached the threshold level $u_{th}$. Only

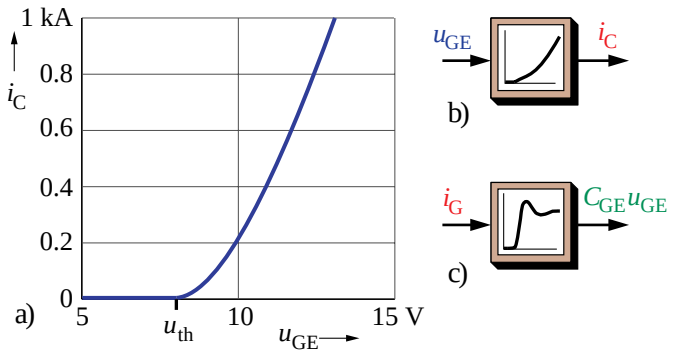


Fig. 4 Characterization of medium voltage IGBTs
(a) static characteristic. $u_{th}$ is the threshold voltage. (b) dynamic behavior at gate *voltage* control, and (c) at gate *charge* control

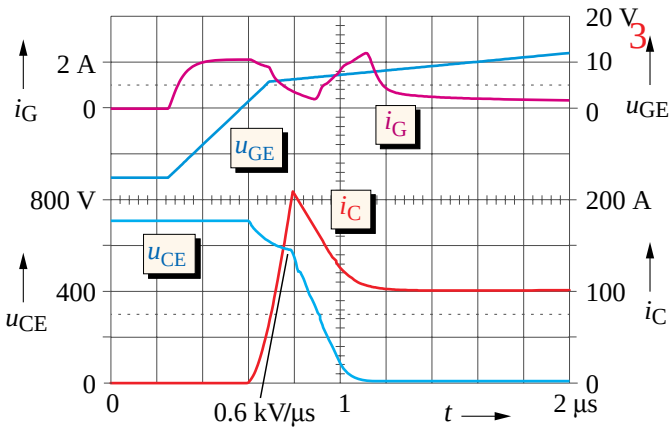


Fig. 6 Turn on process with a voltage ramp $u_{GE}$ applied

then starts the bipolar transistor conducting. A sequence of mutually coupled nonlinear reactions follows: the collector-emitter voltage $u_{CE}$ drops rapidly, which adds to the gate current a displacement current through $C_{GC}$. This capacitance changes as the collector-emitter voltage $u_{CE}$ changes. The current gain of the bipolar transistor depends on the magnitude of the collector current. It is schematically indicated by the step response Fig. 4(c) that the IGBT behaves as a nonlinear higher order oscillatory system.

Earlier investigations of the authors have demonstrated that a low voltage gradient of 0.6 kV/$\mu$s can be achieved without increasing the switching losses [9]. The IGBT was turned on by a ramp-shaped gate voltage having two different gradients as shown in **Fig. 6**. The response shows that the gate current $i_G$ temporarily reduces when the negative gradient of the collector-emitter voltage appears. The effect is owed to a displacement current that is internally injected into the gate through the gate-collector capacitance $C_{GC}$. The result suggests that further research could be worthwhile.

The analysis starts with looking into the IGBT dynamics during switching transitions. The gate current $i_G$ is considered the controlling variable. **Fig. 7** shows the device in the blocking state where the magnitude of the collector-emitter voltage $u_{CE}$ determines the width of the depletion region. This voltage thus controls the gate-collector capacitance $C_{GC}$. Its rapid changes during a switching process results in a fast variation of $C_{GC}$. The dependency

$$C_{GC} = f(u_{CE}) \tag{1}$$

is one of the causes that make the switching dynamics nonlinear. Further nonlinear properties are summarized in the following.

An internal displacement current $\Delta i_G|_1$ caused by changes of $u_{CE}$ is injected into the gate through the gate-collector capacitance $C_{GC}$

$$\Delta i_G|_1 = C_{GC}\frac{du_{CE}}{dt} \tag{2}$$

Another component $\Delta i_G|_2$ that adds to the gate current is the displacement current through $C_{CB}$

$$\Delta i_G|_2 = C_{CB}\frac{du_{CE}}{dt} \tag{3}$$

and hence

$$i_G \neq i_G^* \tag{4}$$

were $i_G^*$ is the commanded gate current.

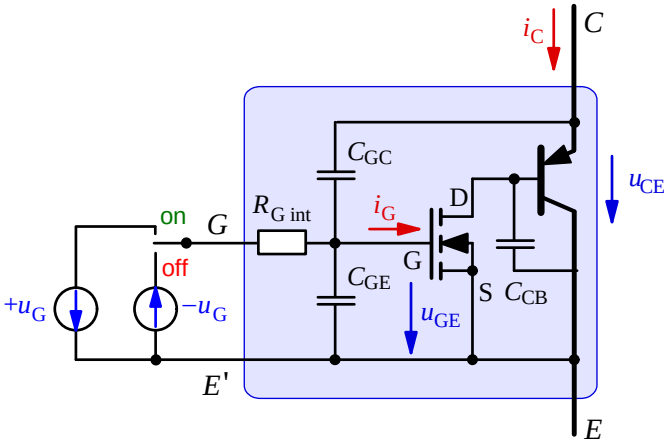


Fig.5 IGBT quivalent circuit

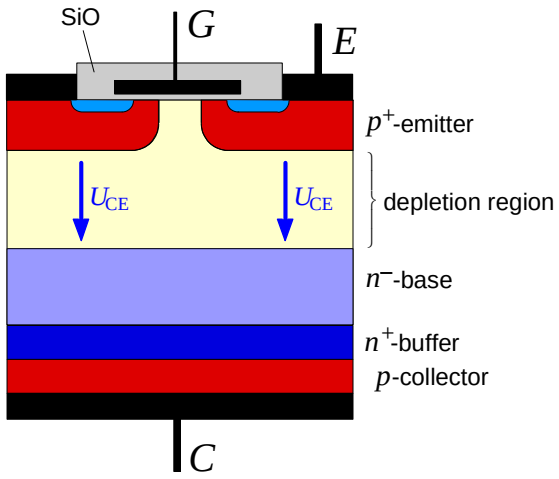


Fig. 7 Structure of an IGBT
The width of the depletion region depends on $U_{CE}$

Fig. 11 Command function at voltage gradient control

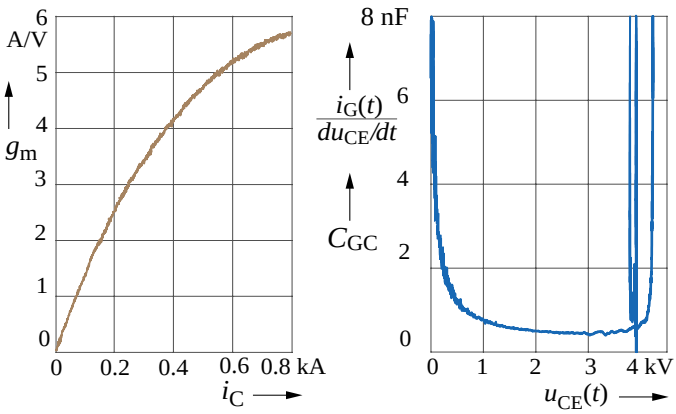


(a) the function $g_m = f(i_C)$ (b) collector gate capacitance

Fig. 8 Identified IBGT characteristics

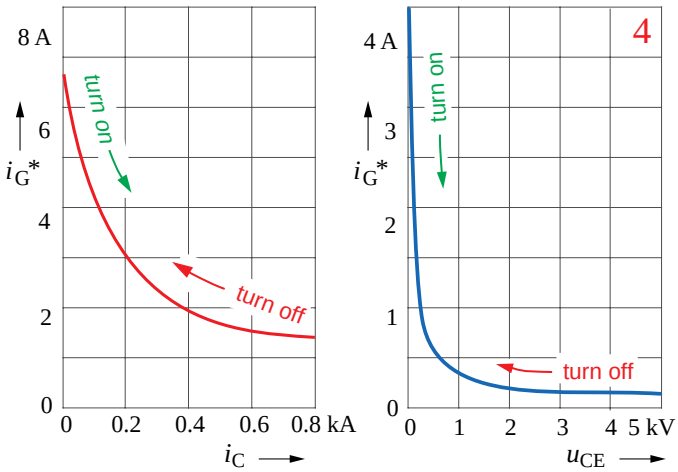


(a) current control (b) voltage gradient control

Fig. 9 Command functions

The gate current $i_G$ changes the gate charge $Q_G$ in the course of time

$$Q_G = \frac{1}{C_{GE}} \int i_G dt \tag{5}$$

which introduces another nonlinearity. $u_{GE}$ is the gate-emitter capacitance. Note that it is the *gate charge* that determines the state of conduction of the MOSFET, not the *gate voltage*.

Finally is the current gain $\beta$ of the bipolar transistor a nonlinear function of the collector current.

$$\beta = f(i_C) \tag{6}$$

Equations (1) through (6) describe the nonlinear dynamics of a medium voltage IGBT. They form part of an algorithm to control the dynamic behavior during the switching process. It is obvious that using the static characteristics alone would not lead to improvement. It is the internal feedback expressed by (1), (2), (3) and (5) that makes the IGBT a higher-order dynamic system.

Operating the IBGT by gate charge control instead of gate voltage control is the basis of a novel method presented here.The strategy is controlling

- at turn on:
  first the current gradient $di_C/dt$
  and subsequently the voltage gradient $du_{CE}/dt$,
- at turn off:
  first the voltage gradient $du_{CE}/dt$
  and subsequently the current gradient $di_C/dt$.

The respective gradients are adjusted by predefined command functions. A constraint is that IGBTs are very fast switching devices. Switching transitions are completed within fractions of a microsecond. The required bandwidth for gate charge control is therefore in the Megahertz range. Traditional methods would not be suited for closed loop control. Event-triggered gate charge control is used instead. The controlling variable is the gate current, derived from command functions that are addressed by the actual dynamic state of the device. The dynamic properties of the respective type of IGBT are identified by measurement. The results serve to deriving the command functions for gradient control.

## III. Event-Triggered Control

### *3.1 Extraction of the command funtions*

The dynamic properties of the IGBT are measured, subjecting the device to a transient condition. A gate current step is applied of constant amplitude $i_G$ =1 Amp. Recorded from the response are the signals

$$g_m(i_C) = C_{GC} \frac{di_C/dt}{i_G} \tag{7}$$

shown in **Fig. 8(a)**, and

$$\frac{i_G}{du_{CE}/dt} = f(u_{CE}) \tag{8}$$

shown in **Fig. 8(b)**.

Since the external gate current is kept constant, it is only the displacement current $\Delta i_G|_1$ through $C_{GC}$ that changes during the transient. Hence the acquired signal (7) permits identifying the gate-cathode capacitance

$$C_{GC}(t) = \frac{\Delta i_G|_1(t)}{du_{CE}/dt} \tag{9}$$

Both the left side term and the right side term of this equation figure at the ordinate axis in Fig. 8(b).

### *3.2 Event driven control at turn on*

Following the turn-on command, the gate current is forced to $i_g$ = 2 A to let the gate charge increase until the emitter voltage $u_{GE}$ has reached the threshold voltage $u_{th}$. This process lasts throughout

$$\Delta t_1 = \frac{Q_G(u_{th})}{i_G} \tag{10}$$

which interval depends on the amount of gate charge $Q_G$ that the device needs to get controllable. $\Delta t_1$ is a device dependent constant interval that triggers event 1 after completion.

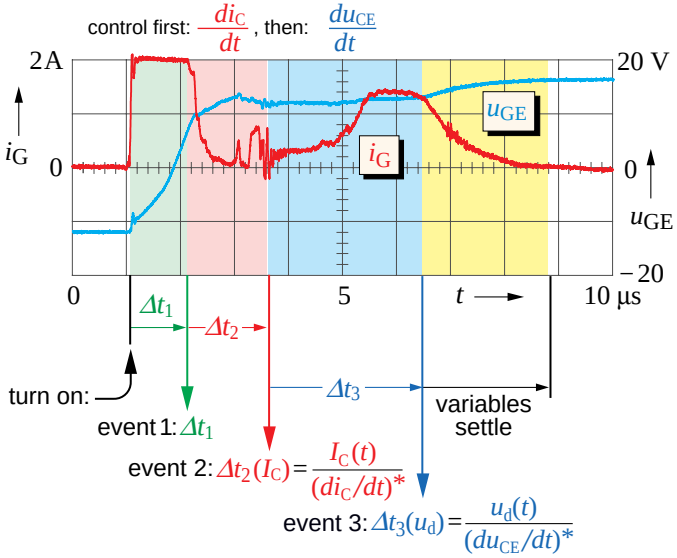


Fig. 10 Event-triggered control at turn on

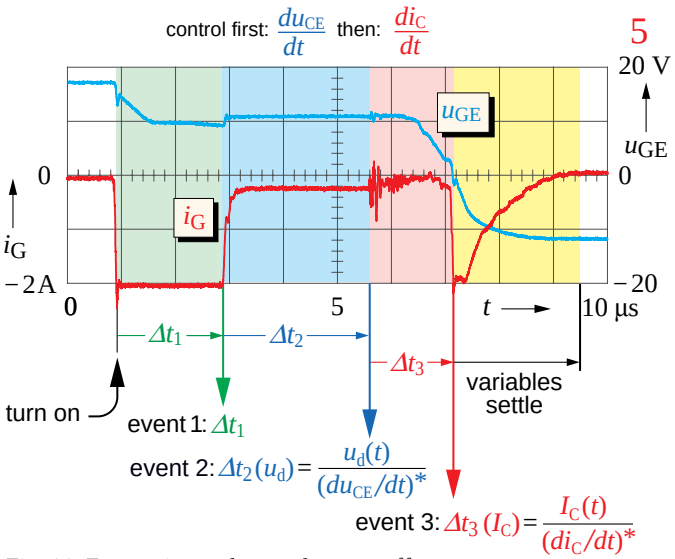


Fig. 11 Event-triggered control at turn off

From this point on the device is controllable.

The gate current reference for current gradient control is now obtained from (7) as

$$i_G^*(t) = \frac{1}{g_m(i_C(t))} C_{GC} \frac{di_C}{dt} \tag{11}$$

This signal is computed from the measured characteristic **Fig. 8(a)**. It defines the command function **Fig. 9(a)** that is stored in a memory. The capacitance $C_{GC}$ in (11) has a constant value since the collector-emittervoltage $u_{CE}$ rests near the dc link voltage $u_d$ at current gradient control. The value of $C_{GC}(u_d)$ is available at **Fig. 8(b)** with the transient oscillations neglected.

The argument $i_C(t)$ in (11) varies rapidly during a switching transient. Measuring its instantaneous value is therefore not possible. A command value ($i_C$-gradient)* is defined onto which the current trajectory is made to follow. The trajectory $i_C(t)$ is computed as

$$i_C(t) = (di_C/dt)^* \cdot \Delta t_2(I_c) \tag{12}$$

It lasts until $\Delta t_2(I_C)$ where $\Delta t_2(I_C) = I_c(t)/(di_C/dt)^*$ is the time required for $i_C(t)$ to reach its maximum value $I_C$ and $(di_C/dt)^*$ is the current gradient command. $\Delta t_2(I_C)$ marks event 2 at which the current ramp is completed. The value $I_c(t)$ is obtained by measurement since it remains almost constant within $\Delta t_2$. Control of the voltage gradient is subsequently initiated.

The oscillations at the end of the commutation in **Fig. 8(b)** are neglected to obtain the clean reference value profile $i_g^*(u_{CE})$ for voltage gradient control, shown in Fig. 9**(b)**. It serves as command function

$$i_G^* = f(u_{CE}(t)) \tag{13}$$

at voltage gradient control and is stored in a table.

The argument $u_{CE}(t)$ of (13) undergoes rapid changes during a switching transient. It cannot obtained by measurement, but since the voltage gradient strictly follows its command value ($u_{CE}$-gradient)*, $u_{CE}(t)$ is computed as

$$u_{CE}(t) = (du_{CE}/dt)^* \cdot \Delta t_3(u_{CE}) \tag{14}$$

where $\Delta t_3(u_{CE})$ is the time required for $u_{CE}(t)$ to reach its final value, which is the dc link voltage $u_d$, and $\Delta t_3(u_d) = u_d(t)/(du_{CE}/dt)^*$ is the voltage gradient command. $\Delta t_3$ marks event 3 at which the voltage ramp is completed. A small residual value is then produced by the command function. It lets the gate voltage rise to its maximum final value, the source voltage of the drive circuit. The gate current decays to zero while the gate-emitter voltage approaches the full source voltage of the drive circuit: the device is locked in its conducting state.

### *3.3 Event driven control at turn off*

Upon receiving the turn-off command, the gate current is forced to $i_g = -2$ A to let the gate discharge the gate until the emitter voltage $u_{GE}$ has come down to the threshold voltage $u_{th}$. $\Delta t_1$ is a device dependent constant interval that triggers event 1 after completion. From this point on the device is controllable.

Gradient control at turn off starts with controlling the voltage gradient. Equation (13) determines the gate current reference with $u_{CE}(t)$, being computed as

$$u_{CE}(t) = (du_{CE}/dt)^* \cdot \Delta t_2(u_d) \tag{15}$$

where $(du_{CE}/dt)^*$ is the voltage gradient command and $\Delta t_2(u_d)$ is the time required for $u_{CE}(t)$ to reach its final value $u_d$. $\Delta t_2$ marks event 2 at which the voltage ramp is completed.

Control of the current gradient follows. Gate current reference (10) is used and $i_C(t)$ is computed as

$$i_C(t) = (di_C/dt)^* \cdot \Delta t_3(I_c) \tag{16}$$

Event 3 at which the current ramp is completed is given as $\Delta t_3(I_C) = I_C(t)/(di_C/dt)^*$. The current reference is now set to – 2A. The gate-emitter voltage then decreases, the gate current reduces to zero, and the device is blocked.

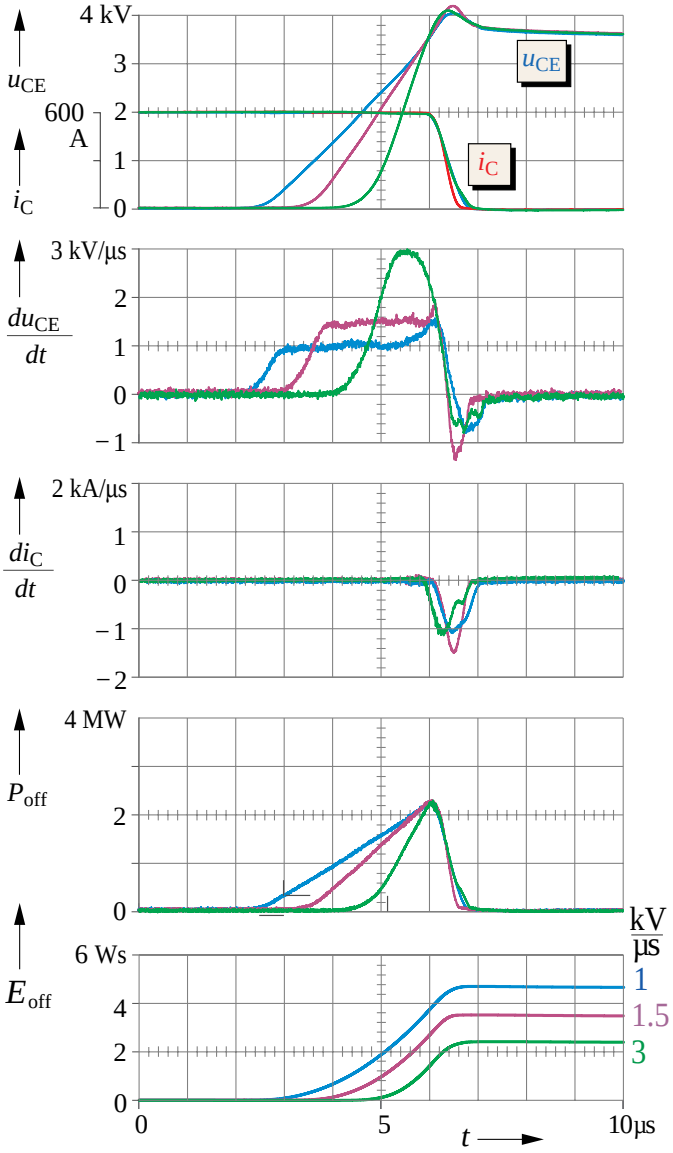


Fig. 12 Event driven control at turn off
command value $(du_{CE}/dt)^*$ = par.

The magnitudes of $I_C$ and $u_d$ during a particular commutation are generally less than the respective maximum values in Fig. 9. It is only portions of the respective command functions that are used.

*3.4 Experimental results*

IGBT type Infineon FZ600R65KF1_S2 was used for experimental verification. The devices were operated at 4 kV dc link voltage and 0.6 kA load current. The command values were set as

$$(di_C/dt)^* = 1\text{kA}/\mu s \tag{17}$$

for current gradient control and

$$(du_{CE}/dt)^* = 1\text{kV}/\mu s \tag{18}$$

for voltage gradient control.

The sequence of events at turn on is shown in **Fig. 10**. Following the turn-on command, the gate current is forced to $i_g$ = 2 A to let the gate charge increase until the emitter voltage $u_{GE}$ has reached the threshold voltage $}_{th}$. This process lasts throughout

$$\Delta t_1 = \frac{Q_G(u_{th})}{i_G} \tag{19}$$

which interval depends on the amount of gate charge $Q_G$ that the device needs to get controllable. $\Delta t_1$ is a device dependent constant interval that triggers Event 1 when $u_{GE}$ has come up to the source voltage of the drive circuit. From this point on the device is controllable. The gate current is then read from the stored command function Fig. 9(a). While the gate charge continues increasing, the collector current starts ramping up. It is kept at the desired gradient $di_C/dt$ = const. according to (17).

The command function Fig. 9(a) is addressed by variable $i_C(t)$, which is computed from (12) to evade time the delays associated to measurement. Depending on the actual range of $i_C(t)$, only portions of the characteristics Fig. 9 are used to address the respective gate current through the time-varying abscissae variable.

Event 2 is computed as $(di_C/dt)^* \cdot \Delta t$, where $(di_C/dt)^*$ is the command value (17) and $\Delta t$ counts the time starting from zero at event 1. Event 2 terminates the range of current gradient control when the collector current has reached the current level $I_C$ of the external load. Since $I_C$ changes only slowly a measured value can be used.

The fly-back diode has now changed to the blocking mode. Its forward voltage starts increasing while the diode capacitance gets charged. The voltage gradient is actively controlled by the IGBT through its gate current reference (18) referring to the command function Fig. 9(b). The time interval $\Delta t_3$ to reach Event 3 is computed as $(du_{CE}/dt)^* \Delta t$ where $(du_{CE}/dt)^*$ is the command value and $\Delta t$ counts the time starting at event 2. Event 3 sets the end to this process when the collector-emitter voltage has reached the level $u_d(t)/(du_{CE}/dt)^*$ where $u_d(t)$ is the measured dc link voltage and $(du_{CE}/dt)^*$ is the command value (18). The gate current continues following its reference (14). It decreases exponentially while charging the gate-emitter capacitance $C_{GE}$ up to the stationary value $u_{GE}$ that equals the source voltage of the gate driver circuit.

A similar sequence of events is used at turn off. The procedure is shown in **Fig. 11**. The turn off command generates a negative current of constant magnitude to discharge the gate-emitter capacitance. During a time interval $\Delta t_1$ is the device transferred to the controllable region using (19). The duration $\Delta t_1$ depends on the gate-emitter capacitance $C_{GE}$ and its charge at the end of the foregoing turn-on process, lastly on the source voltage of the gate driver circuit. The end of this interval defines event 1.

During following time interval the voltage gradient is controlled using the gate current reference (14). Event 2 is computed as $(du_{CE}/dt)^* \Delta t$ where $(du_{CE}/dt)^*$ is the command val-

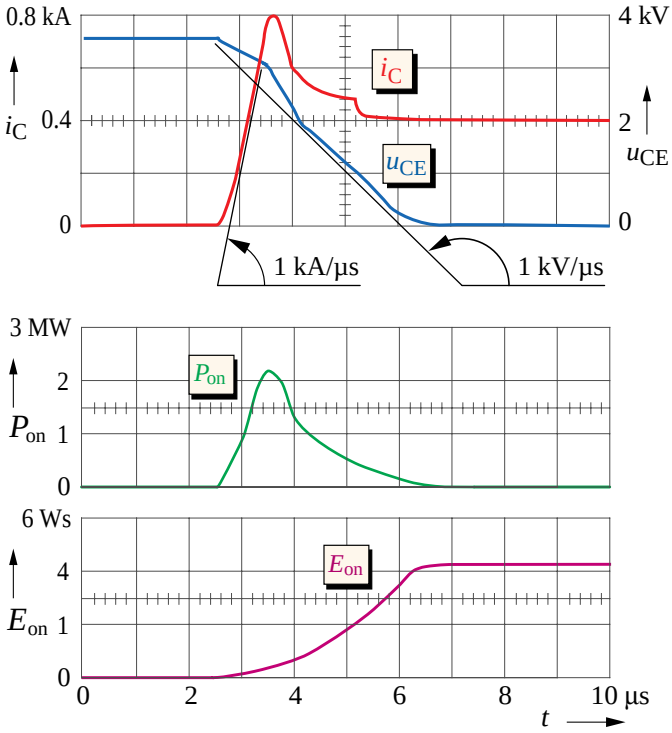


Fig. 13 Event driven control and $R_g$-control at turn on

ue and $\Delta t$ counts the time starting from event 1.

Event 2 terminates the phase of voltage gradient control when $u_{CE}$ has ramped up to the dc link voltage level and the collector current starts from zero.

Control of the current gradient follows. Event 3 that terminates this phase is computed as $I_C(t)/\{(di_C/dt)^*\}$ where $(di_C/dt)^*$ is the command value and $I_C(t)$ is measured. This phase ends when $i_C$ has come to zero.

The turn-off process at event driven control with different settings of $(du_{CE}/dt)^*$ and $(di_C/dt)^*$ is shown in **Fig. 12**. Lower voltage gradients lead to higher the turn-off losses.Turn on at event driven control with $du_{CE}/dt$ = 1 kV/$\mu$s and $di_C/dt$ = 1 kA/$\mu$s is shown in **Fig. 13**. Oscillogram **Fig. 14** shows the performance of voltage gradient control with $du_{CE}/dt$ set to 1 kV/$\mu$s. The gate current waveform results as a smooth signal since the gate drive circuit forces the gate current onto its reference. It compensates the displacement currents that are injected internally into the gate. Against this, there are switching transients being transferred to the gate if conventional gate drive method is used. This method produces more than 4 kV/$\mu$s, **Fig. 15**. Turn-off losses are ccompared in **Fig. 16**, showinga 60% reduction with event driven control. The improvement reduces as the voltage gradient increases. **Fig. 17** shows that it is particularly at lower voltage gradients- that turn-off losses are reduced.

## IV. Summary

Medium voltage IGBTs are fast switching devices. They produce high voltage gradients that generate overvoltages at the connected machines and degrade their bearings. Compensation by AC filters is expensive. Moreover, high current gradients produce high switching losses. These problems are commonly eliminated by limiting the gradients, delaying the switching transitions through added gate registers. The drawback is increasing switching losses and derating of the equipment.

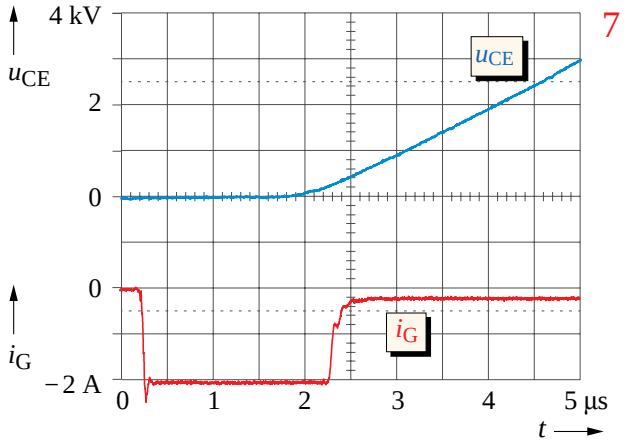


Fig. 14 Turn off at voltage gradient conrol, $du/dt$ = 1 kV/$\mu$s

As a countermeasure, the device is seen as a dynamic system. It is modelled considering the internal cross-couplings between different spatial state variables. To exert an independent control, the forcing variable is not the gate-emitter voltage but the gate current which in turn controls the gate charge. Using this approach, voltage and current gradients are made to follow predefined trajectories. The trajectories are characterized by device-dependent command functions. They are numerically extracted by experiments, stored in a memory and retrieved online. Particular events serve to call the respective command function. The events themselves depend on the respective dynamic state of the device. The method enforces low gradients while reducing the switching losses. It makes additional inverter output filters obsolete.

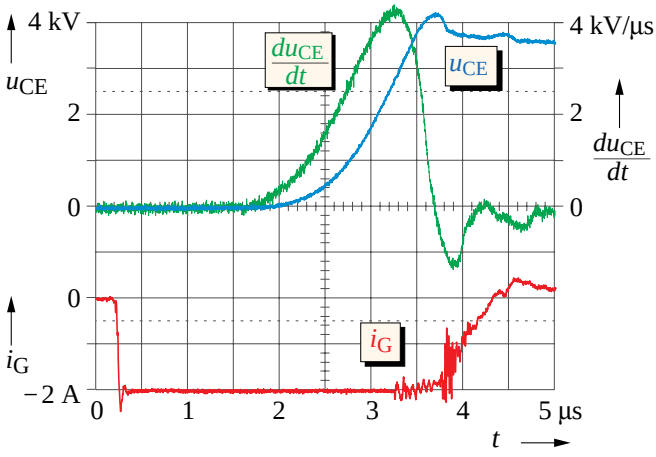


Fig. 15 Conventional turn-off process, $du/dt$ = 4 kV/$\mu$s

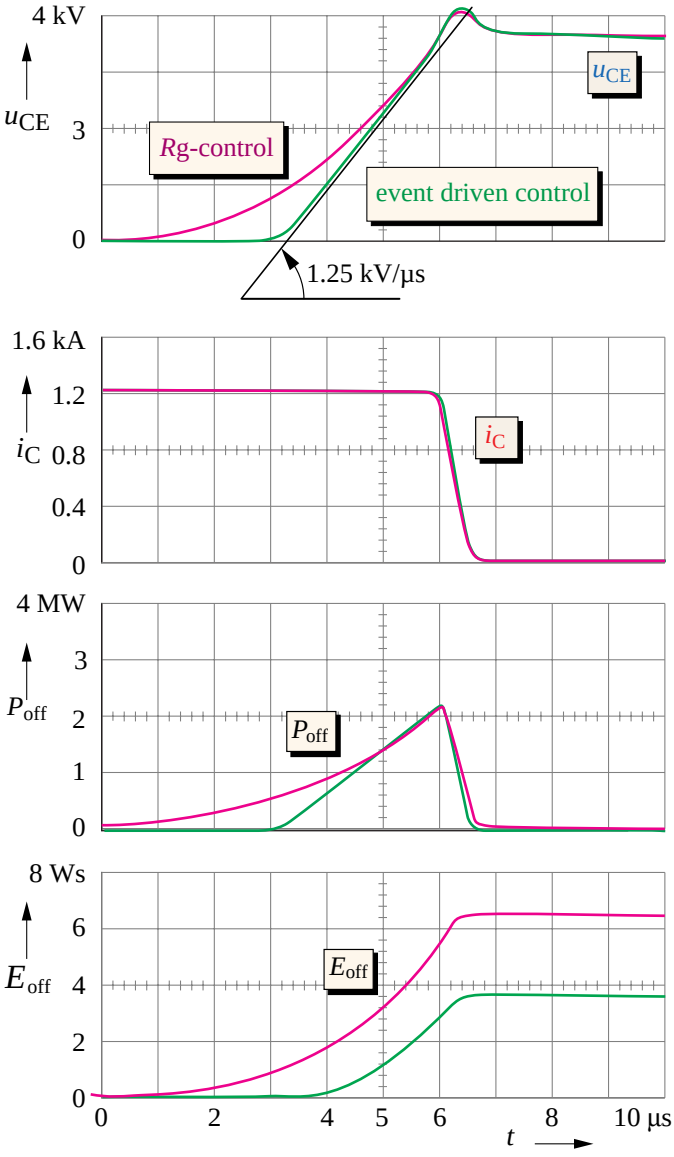


Fig. 16 Comparison: Event driven control and $R_g$-control at turn off

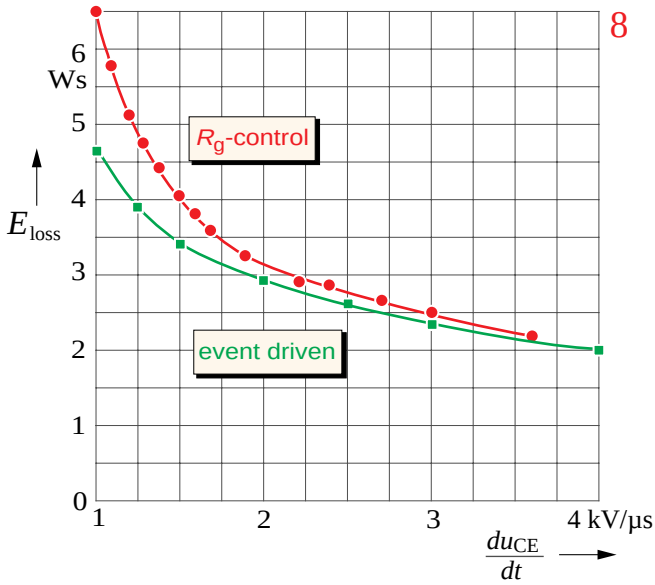


Fig. 17 Conventional and event driven control at turn off

## V. References


1. A. Rathore, J. Holtz, and T. Boller, „Synchronous Optimal Pulsewidth Modulation for Low Switching Frequency Control of Medium-Voltage Multilevel Inverters“, *IEEE Transactions on Industrial Electronics*, 2010, pp. 2374-2381.
2. J. Holtz, G. da Cunha N. Petry, and P. J.Torri, „Control of Large Salient Pole Synchronous Machines using Synchronous Optimal Pulsewidth Modulation“, *IEEE Transactions on Industrial Electronics*, Vol. 62, No. 6, June 2015, pp. 3372-3379.
3. J. Holtz „Advanced Pulsewidth Modulation and Predictive Control – An Overview“, *IEEE Transactions on Industrial Electronics*, Vol. 6?, No. 6, May 2016, pp.
4. T. Boller, A. Rathore, and J. Holtz, „Generalized Optimal Pulsewidth Modulation of Multilevel Inverters for Low Switching Frequency Control of Medium Voltage High Power Industrial AC Drives“, *IEEE Transactions on Industrial Electronics*, Vol. 60, No. 10, 2013, pp. 4215-4224.
5. A. R. Hefner, „An Investigation of the Drive Circuit Requirements for the Power Insulated Gate Bipolar Transistor (IGBT)“, *IEEE Trans. Power Elec.*, Vol. 6, No. 2, April 1991, pp. 208-219.
6. A. R. Hefner, „An Improved Understanding for the Transient Operation of the Power Insulated Gate Bipolar Transistor (IGBT)“, *IEEE Trans. Power Elec.*, Vol. 5, No. 4, Oct 1990, pp. 459-468.
7. T. G. Habetler, R. Naik, and T. A. Nondahl, Design and Implementation of an Inverter Output LC Filter Used for DV/DT Reduction“, *IEEE Trans. Power Elec.*, Vol. 17, No. 3 , May 2002, pp. 327-331.x M. Kojima, K. Hirabayashi, Y. Kawabata, E. C. Ejiogu, and T. Kawabata, „Novel Vector Control System using Deadbeat-Controlled PWM Inverter with Output LC Filter“, *IEEE Trans. Ind. Appl.*, Vol. 9, No. 1, Jan/Feb 2004, pp. 162-169.
8. A. R. Hefner, „Analytical Modeling of Device – Circuit Interactions for the Power Insulated Gate Bipolar Transistor ( IGBT)“, *IEEE Trans. Ind. Appl.*, Vol. 26, No. 6, Nov(Dec 1990, pp. 995-1005.
8. T. Abdelhedi, „Improving the Switching Properties of Insulated Gate Bipolar Transistors (in German)“, Ph.-DThesis, Wuppertal University, 1994.